Thermal properties and crystallization of iron phosphate glasses containing up to 25 wt% additions of Si-, Al-, Na- and U-oxides

Diego O. Russo[a], Diego S. Rodríguez[a], Jesús Ma. Rincón L.[b], Maximina Romero[b], Carlos J.R. González Oliver[a, c, ,]

[a] Centro Atómico Bariloche (CAB), Avenida E. Bustillo 9500, (8400) S. C. de Bariloche, (RN), Argentina
[b] Instituto E. Torroja, CSIC c/ Serrano Galvache 4, Madrid 28033, Spain
[c] Consejo Nacional de Investigaciones Científicas y Técnicas (C.O.N.I.C.E.T) Avda. Rivadavia 1917, CP 1033 AAJ, Buenos Aires, Argentina

Abstract

The thermal properties (expansion, T_g and $T_{SOFT.}$) of glasses, having 56–66% P_2O_5, 14.8–34.2% Fe_2O_3 and 2–25 wt% additions of SiO_2, Al_2O_3, Na_2O and UO_2, were comparatively estimated from dilatometric measurements in similar conditions. The T_g reversibility was clearly verified by varying the heating rates between 1 and 5 °C min^{-1}. From linear equations fits of the various glass properties as functions of the six components it is suggested the iron, sodium and uranium oxides decrease the thermal expansion (for $50 < T \leqslant 300$ °C), T_g and $T_{SOFT.}$ From DTA/XRD analysis of three glasses it was confirmed the crystallization tendency decreased with increasing the UO_2 level in the glasses. Leaching test data for two compositions containing Na_2O suggest addition of UO_2 increases the chemical durability of the related glass. The roles of UO_2, Na_2O and Fe-oxide species as structural components of the glass network are discussed.

PACS

61.43.Fs; 64.70.Pf; 65.60.+a; 61.66.Fn; 67.80.Gb; 28.41.Kw

Keywords

Chemical durability; Crystallization; X-ray diffraction; Glass melting; Glass formation; Glass transition; Glasses; SEM S100; Phosphates; Thermal properties

1. Introduction

Vitrification of industrial wastes has been considered in recent years as a good candidate for inertization and/or recycling of a wide range of wastes [1]. In this sense the vitrification of radioactive wastes is now recognized as the best way for immobilizing isotopes of high and medium activity, resulting from the nuclear power production and applications of nuclear technology in science and industries [2]. Several glassy matrices have been checked and

investigated in the last years by using borosilicate, high silica and lead–iron–phosphate glasses [3] and/or basalt compositions [4], but recently it appeared that iron phosphate glasses are promising matrices for the immobilization of some isotopes [5], [6], [7], [8], [12],[13], [14], [15], [17], [18], [19], [20], [22], [23], [24] and [25]. Thus, Marasinghe et al. [12] had obtained $40Fe_2O_3$–$60P_2O_5$ glasses in the ratios of $Fe^{2+}/Fe_{total} < 0.4$, because over this ratio they had difficulties in making this type of glasses. It seems that they are formed by a network of $Fe^{2+}_{(1-x)} Fe^{3+}_{(x)} (P_2O_7)_2$ groups with clusters of $(Fe_3O_{12})^{16-}$, which are interconnected with the $(P_2O_7)^{4-}$ groups. They depict good durability due to the P—O—Fe bonds, but they crystallize phases like $Fe_3(P_2O_7)_2$ at 650 °C after 24 h of heat treatment. Several X-rays and neutron diffraction, spectroscopical and mechanical resonance studies of these glasses were made to elucidate the structure and to obtain the elastic constants of such glasses [9], [12], [13], [14], [15] and [16]. It appears that the crystallization tendency and kinetics depend strongly on the oxidation states of iron [17], [18] and [19]. In the previous works [20], [22], [23] and [24], various Fe phosphate glasses like M4 ($\sim$61%P_2O_5, $\sim$26%Fe_2O_3) and M5 ($\sim$67%P_2O_5, $\sim$13.2%Fe) containing 13%(SiO_2+Al_2O_3) M4 and 19.7%(SiO_2+Al_2O_3+UO_2) M5 were exploratory melted. Through DTA/TGA in air and XRD it was confirmed that M5 heated up to 800 °C, had a negligible crystallization. At about 507 °C (M4) and 577 °C (M5), the powdered glasses clearly gained weight which was attributed to the oxidation of Fe^{2+} ions. In this work, thermal expansion and T_g/$T_{SOFT.}$ data for six different iron phosphate glasses in the system Na_2O–Fe_2O_3–Al_2O_3–SiO_2–P_2O_5 are reported, with/without additions of U_3O_8. It is aimed at elucidating what may be the effect of varying particular oxide components on such glass properties and how they could be incorporated into the glass structure.

2. Materials and methods

Six original batch compositions listed in Table 1 have been melted in a kanthal furnace model Deltech DT-31 by using sintered alumina crucibles after a previous calcination thermal treatment at 700 °C for 1 h. The melting operation was carried out at 1250 °C in air atmosphere at ambient pressure for 2 h. The liquid batch was poured over a steel mould and the glass pieces were heat treated for releasing stresses at 550 °C followed by slow cooling. The raw materials were $AlPO_4$ (98% pure) and/or $NH_4H_2PO_4$ (99.5% pure) CAAL (Brasil), Fe_2O_3 Berna (Argentina), SiO_2, Na_2CO_3 Cicarelli (Argentina) and U_3O_8 (CAB).

Table 1.   Theoretical and measured chemical compositions of CAB1, CAB2, DR1, DR2, PFeOx and PFeUOx glasses

Composition (wt%)		P_2O_5 (y1)	SiO_2 (y2)	Al_2O_3 (y3)	Fe_2O_3 (y4)	Na_2O (y5)	UO_2 (y6)
CAB1	Nominal	57.51	–	–	42.49	–	–
	Exp. (EDS)	63.42	–	2.43	34.15	–	–
CAB2	Nominal	61.50	–	–	34.08	4.41	–
	Exp. (EDS)	65.81	–	3.30	27.28	3.60	–
DR1	Nominal	55.84	–	–	36.09	–	8.07
	Exp. (EDS)	60.33	–	3.56	30.85	–	5.26
	Fluorescence data plus traces of Cu, Mn, Zn, Cr, Ti, Cl and S	62.7	0.29	2.4	29.4		5.1
DR2	Nominal	54.26	–	–	30.06	–	15.68
	Exp. (EDS)	56.58	–	3.47	26.24	–	13.71
PFeOx	Nominal	60	7	5	20	8	
	Exp. bulk glass (EDS)	62.49	7.61	6.11	16.41	7.37	–
	Exp. glass powder (EDS)	55.31	7.00	8.51	16.78	12.41	–
PFeUOx	Nominal	60	3	3	20	4	10
	Exp. bulk glass (EDS)	59.99	5.69	6.18	14.77	6.41	6.94
	Exp. glass powder (EDS)	58.71	3.17	8.84	14.03	6.76	8.50

The chemical compositions were estimated with a EDS/Edax detector fitted to a SEM Philips 515 scanning electron microscope. The specimens were ground flat and polished with 5 μm diamond paste and the energy data were collected for similar periods of time and maintained the electron current at 20 kV accelerating voltage constant. The data were processed via the standardless mode of the Edax software. The errors in these estimations were about ±2 wt% oxides.The X-rays fluorescence data for DR1 glass were measured with a Bruker SRS3400 apparatus.

The XRD (X-rays diffraction) patterns were measured with a Philips PW 1700 diffractometer at a wavelength of $\lambda_{CuK\alpha} = 1.54054$ Å. The DTA and TGA runs were effected using a Netzsch STA-409 apparatus at a heating rate of 10 °C min^{-1} in static air atmosphere.

The linear thermal expansion (LTE) was measured with a differential vertical dilatometer (Theta Dilatronics II; USA) at heating rates (h) of 5 and 1 °C min^{-1} under oxygen flow. The alumina push rod exerted a 6 g load on the specimen ($L_0 \sim 5$ mm; block of $5 \times 4 \times 4$ mm). The reference was a block of alumina, and the dilatometer was calibrated by inserting a piece of high purity (optical fiber grade) silica glass block of 5 mm in thickness replacing the specimen and repeating the thermal cycle. The corrected data are quoted as $\Delta L/L_0 = [L(T) - L_0]/L_0$, where L_0 is

the initial height of the specimen. The errors in $\Delta L/L_0$ and T measurements are less than 3% and $\pm$ 3 °C, respectively.

3. Results

3.1. Glass melting, chemical compositions and leaching tests

The glass compositions quoted in Table 1 as [Exp.(EDS)] were estimated via EDS/SEM in the same conditions for all the glasses, making a comparative analysis of the effect of composition on the physico-chemical properties among the glasses possible. Even though, for PFeOx and PFeUOx some variations are noted in the analysis when the values for flat polished glass are compared to those for glass grains. Furthermore, it is noted that the fluorescence analysis gave 2.4 wt% more P_2O_5, 1.4% less Fe_2O_3, 1.1% less Al_2O_3 and 0.2% less UO_2 than the EDS [Exp.(EDS)]-analysis for DR1 glass. Comparing the theoretical batch compositions with the measured ones, it is clear that some losses of Fe_2O_3 and UO_2 occurred during melting. It is also clear that alumina was incorporated to the original glasses due to crucible corrosion in all glasses in proportions between 2.4 and 3.6 wt%. Consequently, the analysis is affected by this addition, decreasing the Fe_2O_3 contents and increasing the Al_2O_3 content. For the phosphate glasses containing Na_2O, some losses in Na_2O were obtained due to some volatilization, except for PFeUOx. This more complex glass PFeUOx, with six starting oxide components, increased its alumina level due to the crucible corrosion and decreased the UO_2 content in the final glass affecting the values for the other components. The glass densities for the uranium containing glasses were 3.044 (DR1), 3.204 (DR2) and 2.964 g cm^{-3} (PFeUOx).

The final measured glass compositions have P_2O_5 and Fe_2O_3 contents ranging between 56% and 66% for P_2O_5 and between 14.8% and 34.2% for Fe_2O_3. These compositions may be tentatively regarded as P-/Fe-oxides matrices containing between 2 and 25 wt% additions of the remaining oxides in Table 1. Such additions were 2.43% Al_2O_3 CAB1, 6.9% (Al_2O_3+Na_2O) CAB2, 8.8% (Al_2O_3+UO_2) DR1, 17.2% (Al_2O_3+UO_2) DR2, 21.1% (SiO_2+Al_2O_3+Na_2O) PFeOx and 25.2% (SiO_2+ Al_2O_3+Na_2O+UO_2) for PFeUOx. It is of interest to note that the ionic crystal radii (Å) for coordination number CN = 6 for the components present in these glasses are about P^{5+} 0.35, O^{2-} 1.40, Si^{4+} 0.40, Fe^{2+} 0.77, Fe^{3+} 0.65, U^{4+} 0.89–0.97, U^{5+} 0.79, Al^{3+} 0.53 and Na^+ 1.02 [10] and [11]. Therefore, for example, U^{4+} ions could be located in sites replacing Na^+ ions. It has been proposed for iron phosphate glasses (containing about 40 mole% Fe_2O_3) showing enhanced chemical resistance towards aqueous corrosion that the P_2O_7 groups are joined by Fe^{3+} in tetrahedral/octahedral oxygen coordination [12], [13], [14], [15] and [25]. The

larger Fe^{2+} in octahedral coordination would be located between the chains formed by PO_4 groups and Fe^{3+} polyhedra, and so the Fe^{2+} ions can be considered as network modifiers. The enhanced chemical resistance is attributed to the formation of Fe—O—P bonds.

As noted above these iron phosphate glasses are of interest since high dissolution power of, for instance, uranium oxide has been confirmed and that such charged matrices can be reasonably stable towards aqueous corrosion. In Fig. 1 are shown leaching tests[20] and [21] for PFeOx and PFeUOx glasses having, respectively, 16.41 and 14.77 wt% Fe_2O_3. The rough parabolic fits were made only as guides to the eye. The lower leaching rate for PFeUOx as compared to that for PFeOx is noted. The main difference between the Exp.EDS compositions of these two glasses is that PFeUOx contains about 7 wt% UO_2 (Table 1), and this suggests that additions of UO_2 increase the chemical durability of such complex glasses. This confirms the idoneity of this type of glassy matrices for the immobilization of uranium, though the relative stability in water is not probably high enough for the final recommendation of this matrix for retention of this element from radioactive wastes [5].
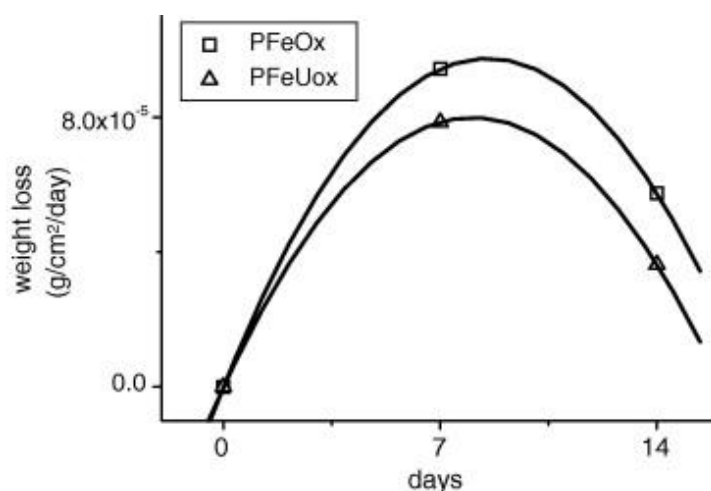

Fig. 1. Leaching (PTC) essays for PFeOx and PFeUOx glasses.

3.2. XRD/DTA/TGA

In Fig. 2 are shown the XRD curves for all the glasses except for PFeOx which was not determined. They are all amorphous and if carefully observed it appears that some scattering differences exist in both ranges (a) 24–25° and (b) 40–80° when CAB1/CAB2 (compositions not containing uranium) are compared to DR1/DR2/PFeUOx glasses.
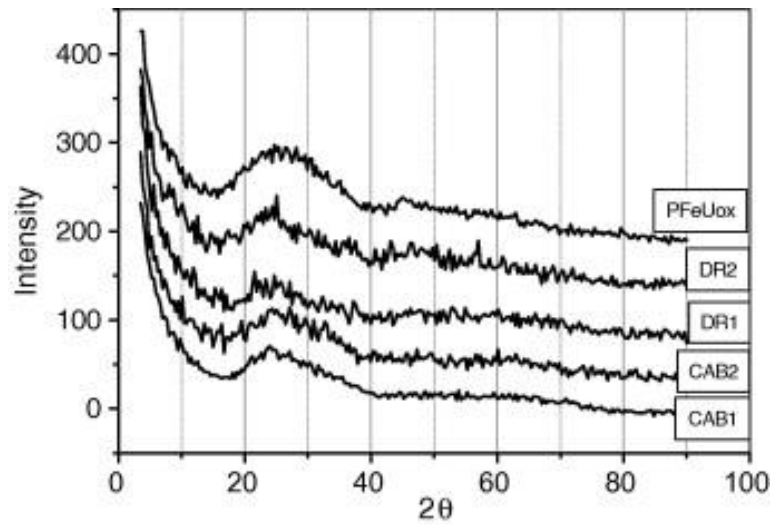
Fig. 2. XRD data for powdered CAB1, CAB2, DR1, DR2 and PFeUOx glasses.

For these iron–phosphate glasses, in fine powder form, it is not always possible to obtain clear DTA traces (for O_2-containing atmospheres), with well-defined endothermic or exothermic peaks, perhaps owing to the fact that for certain compositions they are indeed difficult to be crystallized [20] and [22]. In Fig. 3 and Fig. 4 are shown the best traces obtained for CAB1 and DR1. In both the cases the endothermic peak corresponding to T_g was made clear by over imposing the dilatometric curve (see later) of each glass into the graph.
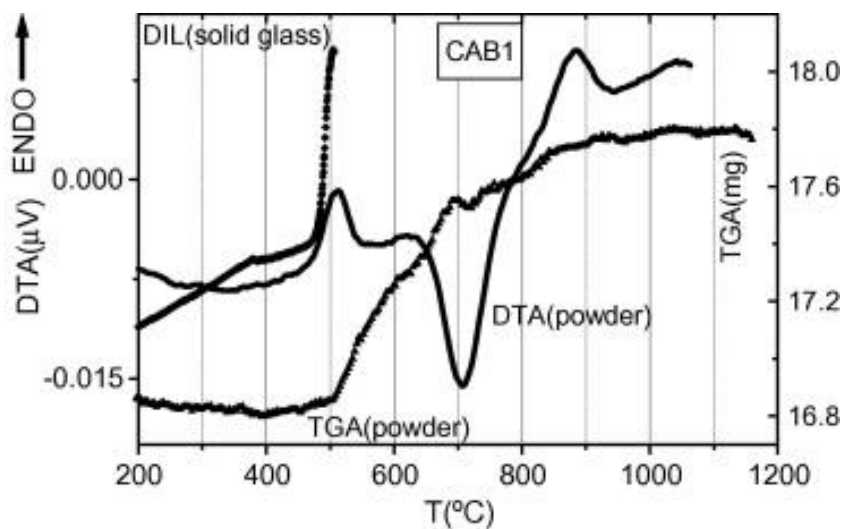

Fig. 3. DTA/TGA runs at 10 °C min^{-1} in air for CAB1 in powder form, and dilatometric curve (at 5.3 °C min^{-1}) for solid glass CAB1.
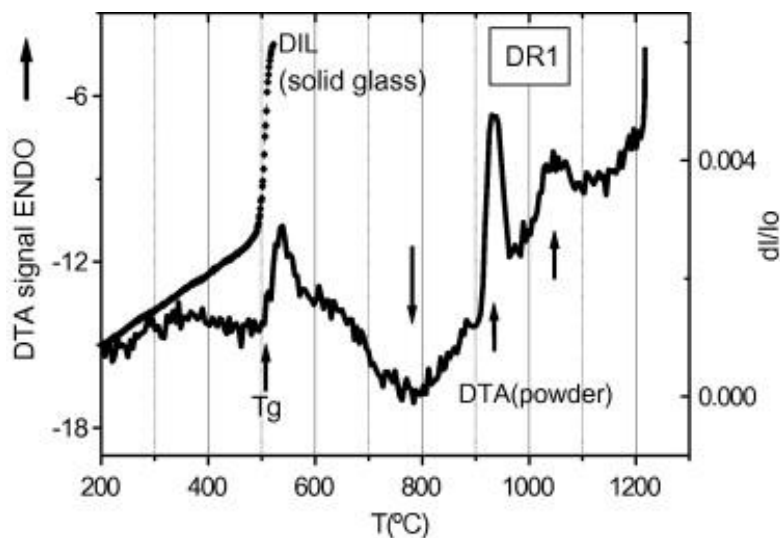
Fig. 4. DTA run (10 °C min^{-1}) in air and dilatometric curve (at 5.2 °C min^{-1}) under O_2 flow for glass DR1.

For CAB1 it is clear enough that after about 650 °C the glass started to crystallize with exothermic peak-minimum at around 700 °C and that the precipitated phase (s) melted with endothermic peak-maximum at around 880 °C. For CAB1 it is also of interest to note that for $T \geqslant T_g$ and more precisely for $T \geqslant 520$ °C the TGA curve shows very clearly that the glass started gaining weight. This could well correspond to the oxidation of Fe^{2+} ions into Fe^{3+}ones, as marked in [18] where for similar glasses (melted in air atmosphere for different temperatures and periods of time) the contents of both ions were measured via Mossbauer spectroscopy. For DR1 the crystallization peak-minimum is met at around 783 °C and two melting peaks are obtained at 934 and 1045 °C (see the arrows in Fig. 4). DR1 contains 1.2% more Al_2O_3, 5.3% more UO_2 and 3.3% less Fe_2O_3 than CAB1 and these compositional variations are taken as those responsible for the delayed crystallization detected for DR1 as compared to that for CAB1. Futhermore, for DR1 and DR2 heated up to about 780 °C, the XRD traces (not shown here) showed the presence of $Fe_2Fe(P_2O_7)_2$(JCPDS 80-2315) and $U(PO_3)_4$ (JCPDS 25-0997) in the bulk of the glasses. On the surfaces of the partially crystallized glasses, the crystalline phase $Fe(PO_3)_3$ (JCPDS 38-0109) was detected in addition to the two phases mentioned previously. The crystalline peak intensities for DR1 were slightly stronger than those for DR2. It should then be noted that at least part of the uranium component dissolved in the glass structure may be precipitated as, for instance, phosphate compounds and that the temperatures of the crystallization peaks can depend strongly on the UO_2 level in the glasses.

3.3. Thermal expansion properties [T_g, $T_{SOFT.}$ and linear thermal expansion (LTE)]

In Fig. 5, Fig. 6 and Fig. 7 are shown the LTE curves for the six glasses. The glass pieces were initially (T1) heated to $T_{SOFT.}$ at 5.3–5.5 °C min^{-1}, (T2) cooled down to room temperature at 1 °C min^{-1} and (T3) heated rapidly (5.2–6.2 °C min^{-1}) up to 400 °C and finally continued the heating from 400 to $T_{SOFT.}$ at 1 °C min^{-1} (T4).
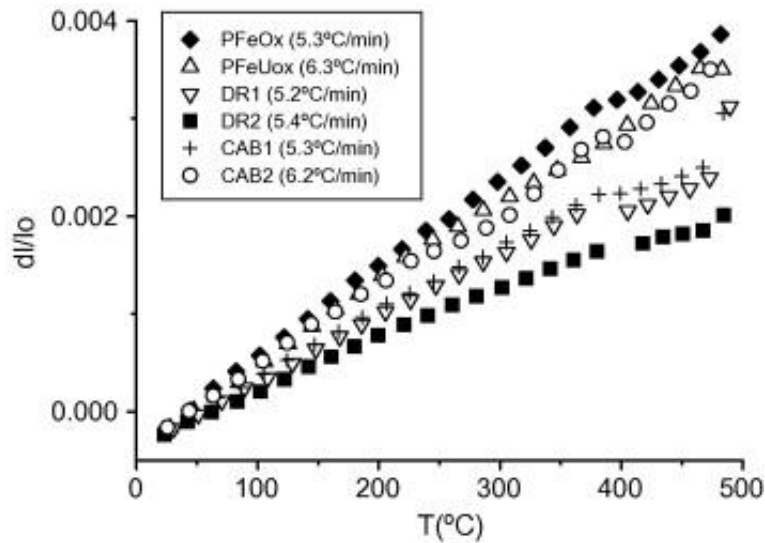
Fig. 5. Thermal expansion of glasses PFeOx, PFeUOx, DR1, DR2, CAB1 and CAB2 up to 500 °C under O2 flow at 5.2–6.3 °C min^{-1} heating rate. This corresponds to heat treatment T3 (see the text).

Fig. 6. Thermal expansion of glasses PFeOx, PFeUOx, DR1, DR2, CAB1 and CAB2 from 400 °C up to TSOFT. under O_2 flow at 5.3–5.5 °C min^{-1} heating rate. It corresponds to heat treatment T1 (see the text).
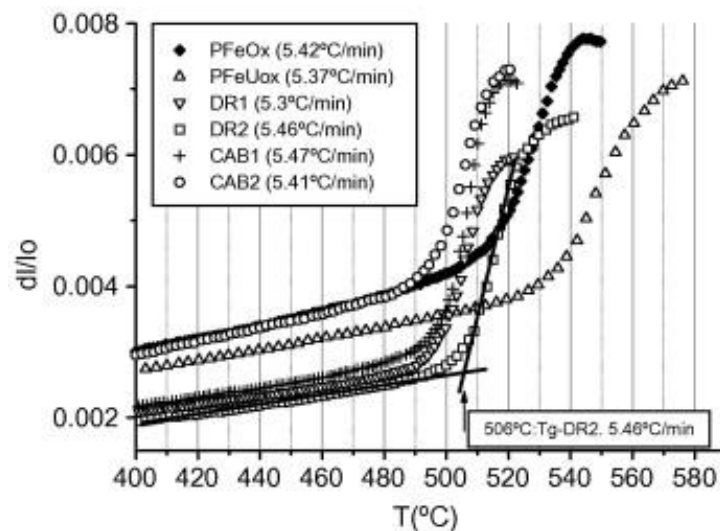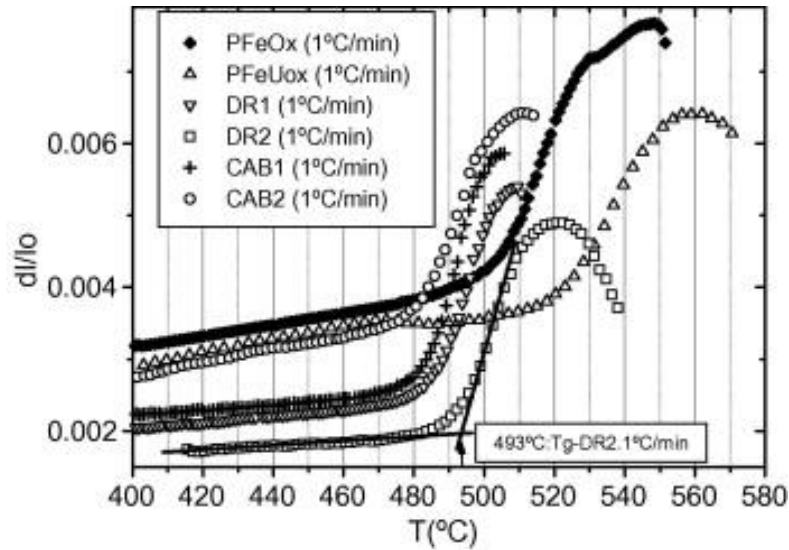
Fig. 7. Thermal expansion of glasses PFeOx, PFeUOx, DR1, DR2, CAB1 and CAB2 from 400 °C up to TSOFT. under O_2 flow at 1 °C min^{-1} heating rate. This corresponds to heat treatment T4 (see the text).

It is quite evident that after a more or less linear expansion up to roughly 480–520 °C (depending on glass composition and heating rate; note also the change from cycle T3 to T4 at around 400 °C in Fig. 5), the LTE increases very markedly in the glass transition or transformation range. The linear thermal expansion coefficient α is defined as $\alpha = (\Delta L/L_0)/\Delta T$, where ΔT corresponds to the temperature range of the measurement. The coefficient α was estimated from the slope of lines interpolating the $\Delta L/L_0$ data (Table 2), and T_g (glass transition temperature) was estimated from the intersection of the two lines (for the low and high T (°C)-ranges) drawn as shown for glass DR2 in Fig. 6 and Fig. 7. From these curves in the glass transformation range, it may be advanced that the glasses behave as expected concerning the T_g reversibility. That is, with increasing h the apparent T_g shifts to higher temperature and conversely. The dilatometric softening points or temperatures, $T_{SOFT.}$, correspond to the maxima shown in Fig. 6 and Fig. 7 (Table 2).

In Fig. 5 are shown the LTE curves for T3 cycle, and the α-values (Table 2) for the glasses are found to be in between those for PFeOx and DR2. It may be noted that the values $\Delta L/L_0(T(°C))$ for CAB1, DR1 and DR2 are slightly curved downward, whereas those for PFeOx, CAB2 and PFeUOx oscillate around a straight line. In Fig. 7 are shown the $\Delta L/L_0$-data in the glass transformation range, for $h = 1$ °C min^{-1} (cycle T4) for the same specimens (Fig. 5 and Fig. 6), which were cooled in the dilatometer at 1 °C min^{-1}.

Table 2. Expansion coefficient α, T_g and $T_{soft.}$ values for CAB1, CAB2, DR1, DR2, PFeOx and PFeUOx glasses

Code	$\alpha[\times10^{-7}(°C^{-1})]$	T_g (°C) 5.3-5.5°C/min;T1	T_g (°C) 1°C/min;T4	$T_{soft.}$ (°C)
CAB1	67.10 [50–400 °C, 5.3 °C/min],T3;∗67.39 [50–300 °C, 5.3 °C/min], T3;	500		520, 5 °C/min, T1
	36 [400–470 °C, 1 °C/min], T4		483	504, 1 °C/min, T4
CAB2	78.20 [50–400 °C, 6.2 °C/min], T3;∗83.94 [50–230 °C, 6.2 °C/min], T3;	496		520, 5 °C/min, T1
	87.1 [400–470 °C, 1 °C/min] , T4		482	510, 1 °C/min, T4
DR1	65.30 [50–400 °C, 5.2 °C/min], T3;∗65.97 [50–300 °C, 5.2 °C/min], T3;	497		521, 5 °C/min, T1
	45 [400–470 °C, 1 °C/min], T4		486	508, 1 °C/min, T4
DR2	52.40 [50–400 °C, 5.4 °C/min], T3;∗57.24 [50–210 °C, 5.4 °C/min], T3;	506		541, 5 °C/min, T1
	28 [417–470 °C, 1 °C/min], T4		493	519, 1 °C/min, T4
PFeOx	90.40 [50–400 °C, 5.3 °C/min],T3;∗90.14 [50–300 °C, 5.3 °C/min],T3;	515		546, 5 °C/min, T1
	79 [400–470 °C, 1 °C/min], T4		503	531–547, 1 °C/min,T4
PFeUox	84.70 [50–400 °C, 6.3 °C/min],T3;∗87.52 [50–300 °C, 6.3 °C/min],T3;	535		578, 5 °C/min, T1
	88–94 [400–470 °C, 1 °C/min], T4		523–526	559, 1 °C/min, T4

For cycle T3, the three compositions: CAB1, DR1 and DR2, have close expansivities grouped in the range of the lower α-values among the glasses, and it could be suggested that such glasses have similar glass structures. It is clear that αCAB1 $\approx$ αDR1 > αDR2 and that for this series the P_2O_5 and Fe_2O_3 contents decrease and the UO_2 level increases nearly monotonically (Table 1). Although α for CAB2 is clearly larger than that for CAB1, their (T_g; $T_{SOFT.}$; Table 2) values were quite similar. For cycle T4 (for $T \geqslant 400\,°C$ and a heating rate of $1\,°C\,min^{-1}$) also αCAB1 $\approx$ αDR1 > αDR2, confirming somehow that these glasses have similar structures. However, the origin of the drop in the expansion coefficient for $T \geqslant 400\,°C$ for these glasses is not yet known.

As noted above, the compositional variations of these glasses as well as their expansion and $T_g/T_{SOFT.}$ behaviors are indeed quite large and it is difficult to elucidate any trend in properties caused by individual glass-components. There exists some collection of thermal expansion data for more or less similar glasses [25], [26] and [27], but it is somehow difficult to extrapolate and compare such values to the ones estimated in this work. For sodium–iron phosphate glasses, it was obtained that with increasing Fe_2O_3 and Na_2O contents the dilatometric softening temperature increased and the thermal expansion coefficient and dissolution in H_2O at $90\,°C$ decreased [25].

Let us examine these effects in terms of linearly fitting α, T_g and $T_{SOFT.}$ to the six glass compositions taken as weight fractions. Using Cramer´s rule, the system of six equations with six variables can be solved. The α-values marked with * in Table 2 estimated in the range 50–210/300 °C for the data collected during cycle T3 at 5.2–6.3 °C min^{-1} were used. The values for cycle T1 (Fig. 6) were used for the calculations of the dependencies of T_g and $T_{SOFT.}$ with composition. As a result, Eqs. (1), (2) and (3) were obtained.

$$\alpha = (4.4289 \times 10^{-5} * y1) + (-2.1989 \times 10^{-5} * y2) + (3.8843 \times 10^{-5} * y3) + (-6.5289 \times 10^{-5} * y4) + (-11.7303 \times 10^{-5} * y5) + (-2.5917 \times 10^{-5} * y6) \tag{1}$$

$$T_g = (3324.0802 * y1) + (649.7220 * y2) + (-296.1695 * y3) + (-4688.6559 * y4) + (-11181.2372 * y5) + (-980.1777 * y6) \tag{2}$$

$$T_{SOFT.} = (4157.3949 * y1) + (671.0017 * y2) + (-536.5176 * y3) + (-6160.734 * y4) + (-14370.6262 * y5) + (-1286.0233 * y6) \tag{3}$$

For example, the (α, T_g) values for CAB1 and $T_{SOFT.}$ for PFeUOx may be obtained through the following expressions:

$$\alpha_{CAB1} = (4.4289 \times 10^{-5} * 0.63423) + (3.8843 \times 10^{-5} * 0.0243) + (-6.5289 \times 10^{-5} * 0.34147) = 67.39 \times 10^{-7} (°C^1)$$

$$
\begin{aligned}
T_{gCABI} &= (3324.0802 * 0.63423) + (-296.1695 * 0.0243) \\
&\quad + (-4688.6559 * 0.34147) \\
&= 500°C, \text{ and, } T_{gSOFT.PFeUOx} \\
&= (4157.3949 * 0.59993) + (671.0017 * 0.05692) \\
&\quad + (-536.5176 * 0.06184) + (-6160.734 \\
&\quad * 0.14773) + (-14370.6262 * 0.06414) \\
&\quad + (-1286.0233 * 0.06944) \\
&= 578°C
\end{aligned}
$$

From Eqs. (1) and (2), the very strong influence of Na_2O content on both α and T_g is noted. This contribution is negative for α and T_g. The second more important contribution comes from the Fe_2O_3 content, being also negative for α and T_g. Concerning α, the third influence is shared between the P_2O_5 and Al_2O_3 contents which are both positive: i.e. the coefficient of thermal expansion is increased with the increase of such components. The P_2O_5 content is also the third contribution to T_g and it is positive. It is of interest to note that additions of UO_2 decrease both α and T_g, in the same way as Na_2O and Fe_2O_3 do, but to a lesser extent. In summary, it can be suggested tentatively that α is increased by P_2O_5 and Al_2O_3 additions and it is decreased by Na_2O, Fe_2O_3, UO_2 and SiO_2. T_g is decreased by Na_2O, Fe_2O_3 and UO_2 additions and it is increased by P_2O_5 and SiO_2; the influence of Al_2O_3 is negligible. The trend for $T_{SOFT.}$ is approximately similar to that for T_g.

The behavior of these six glasses in the transformation range is as expected for 'normal' silicate glasses exhibiting no phase-separation effects. That is, by decreasing the heating rate the T_g values decrease and the shapes of the $\Delta L/L_0$ vs. T (°C) curves are similar for both h of ~5 and 1 °C min^{-1}. These curves (see Fig. 6 and Fig. 7) are smooth from T_g to $T_{SOFT.}$ with the exception of that for PFeOx at 1 °C min^{-1}, which shows a short plateau at about 530 °C before $T_{SOFT.} \sim 548$ °C. The origin of such an effect for this composition is not yet known.

Attempting to clarify the type of glassy structure these glasses may have, it is relevant to study the behavior of these compositions also in the range from T_g to $T_{SOFT.}$, where a more

'liquid-like' character would be expected. The slopes of the $\Delta L/L_0$ curves after the T_g break do change very markedly for these glasses (Fig. 6 and Fig. 7). The calculated values for T1 cycle (Fig. 6) were 253.644×10^{-6} (CAB1, 500–514 °C), 169.644×10^{-6} (CAB2, 500–514 °C), 168.106×10^{-6} (DR1, 500–514 °C), 172.904×10^{-6} (DR2, 505–525 °C), 131.122×10^{-6} (PFeOx, 517–539 °C) and 93.212×10^{-6} °C^{-1} (PFeUOx, 534–564 °C). Again a 6×6 linear system may be solved using these new expansion independent terms and the following Equation was obtained:

$$\alpha = (1.9217 \times 10^{-3} * y1) + (2.7684 \times 10^{-3} * y2) + (-7.1135 \times 10^{-3} * y3) + (-2.3202 \times 10^{-3} * y4) + (-6.3110 \times 10^{-3} * y5) + (-0.4291 \times 10^{-3} * y6) \tag{4}$$

$$\text{For example}: \alpha_{CABI} = (1.9217 10^3 * 0.63423)$$
$$+ (-7.1135 10^{-3} * 0.0243)$$
$$+ (-2.3202 10^{-3} * 0.34147)$$
$$= 253.66 \times 10^{-6} (^{\circ}C^{-1})$$

The negative influences of Al_2O_3 (very strong), Na_2O (strong) and Fe_2O_3 (mild effect) on the expansion in the range $T_g < T < T_{SOFT.}$ are noted; the contribution of UO_2 is negligible. The positive contributions are for P_2O_5 and SiO_2. Some of these effects are the opposite when compared to those for the glassy solid like α in the $T < T_g$ range. Therefore, it appears that when the ion movements are triggered on (for $T > T_g$), the behavior of the liquid is now significantly different when compared to that of the glass. The lowest apparent expansion obtained for PFeUOx liquid could be attributed to the strong glass complexity given by the 25.2% additions (to the P-/Fe-oxide matrix) of the other oxides; the main influences are given by the high Al_2O_3 and Na_2O levels in the glass.

4. Discussion

Although these glass melts are reasonably fluid at 1200–1400 °C in air, making it possible to cast them properly, they exhibit losses of some compounds like Fe_2O_3 and UO_2 and furthermore, they corrode nearly any oxide crucible used for melting [3] and [7]; note in [16] the authors mentioned that xFe$_2$O$_3$– $(100−x)$P$_2$O$_5$ glasses were melted in covered Pt-crucibles. Recent melting trials in our laboratory, at about 1250 °C in air using alumina crucibles, gave only 75 wt% of glass (contaminated with Al_2O_3) as compared to the initial batch. The remaining

25% of glass in the crucible could only be removed by fluxing with K-nitrate/hydroxides at about 1000 °C. These effects imply difficulties in obtaining the exact chemical composition variations for systematic studies. Also, as mentioned above, there are significant differences in chemical compositions between fluorescence and EDS data and it is recalled that acceptable chemical analysis data are needed for exact comparisons or predictions. Furthermore, as shown in detail [17], [18], [19], [20] and [22], the ratio Fe^{2+}/Fe^{3+} can vary strongly depending on the melting temperature and time and on the glass composition. As these effects strongly control the crystallization kinetics, it is also important to precisely maintain the temperature, time and the O_2-content over the melt before casting the related glasses.

The water-leaching tests [21] are of interest, but however, to better define the chemical resistance of such glasses full chemical durability assays should be performed. Comparing PFeUOx, with PFeOx, the increased durability of the former can be associated to the larger addition of 25.2% of extra oxides (with particular emphasis to the UO_2 content) increasing the glass complexity as compared to that for PFeOx. It should also be noted that PFeUOx may possess a stronger structure than PFeOx, as evidenced by the lower α and higher$T_g/T_{SOFT.}$ (Table 2; Fig. 5, Fig. 6 and Fig. 7) and the lower expansion for $T > T_g$. The leaching test for PFeUOx gives roughly twice as much ion concentration in the leachate when compared to roughly similar phosphate glasses or ARM-1 reference borosilicate glass [5]. However, it can be proposed that substantial improvements could be reached by modifying the PFeUOx composition, as it can be the case after replacing some of the Na_2O with Fe_2O_3, Al_2O_3 or UO_2. Furthermore, these glasses containing U-oxide should also be tested after heating in oxidizing atmospheres up to about 700 °C since in that way the Fe^{2+} ions are oxidized to Fe^{3+} and remain in that ionic form (probably due to the presence of U ions) after cooling to room temperature [22]. The glass durability can benefit from this since it has been noted that for higher Fe^{3+}/Fe^{2+} ratios the chemical durabilities of iron–phosphate glasses increase [12].

As reported for CAB1, DR1 and DR2, the crystallization tendency appears to decrease by reducing the ($P_2O_5+Fe_2O_3$) levels: 97.57 wt% CAB1, 91.18% DR1 and 82.82% DR2, and increasing the additions of the remaining oxides: 2.43% (Al_2O_3) CAB1, 8.8% ($Al_2O_3+UO_2$) DR1 and 17.2% ($Al_2O_3+UO_2$) DR2.

It is not known as to what crystalline phase (s) precipitated in CAB1 at $T \leqslant 700$ °C but such a phase apparently melted at $T \leqslant 880$ °C. For a glass 31 mol% $Fe_2O_3 \cdot 69\% P_2O_5$, crystallizations at $T \leqslant 640$ °C and at $T \leqslant 800$ °C of, respectively, $Fe_3(P_2O_7)_2$ and $Fe_4(P_2O_7)_3$[12] were obtained. Then, for CAB1 it could be possible it crystallized also $Fe_3(P_2O_7)_2$ such as the higher T obtained

in the present work can be related to the $2.43\% Al_2O_3$ in the glass. Such crystal phase $Fe_3(P_2O_7)_2$ should contain $1Fe^{2+}$ and $2Fe^{3+}$ sites. For CAB1 (initial mass of 17 mg) from the TGA curve in Fig. 3, and assuming that the weight-gain at $T \geqslant 520\,°C$ (amounting to ~ 1 mg) is due to the oxidation of Fe^{2+} (into Fe^{3+} ions), $17\%\ Fe^{2+}$ and $83\% Fe^{3+}$ can be calculated thus supporting the possibility that $Fe_3(P_2O_7)_2$ was precipitated in CAB1. The DTA run for CAB1 is also close to that for glass F–30–H (70 mol% $P_2O_5 \cdot 28\%\ Fe_2O_3 \cdot 2\%\ Al_2O_3$), which showed crystallization and melting peaks (DTA run under argon flow) at, respectively, 695 and 845 °C [17], temperatures close to the ones in Fig. 3.

For glasses based on 60 mol% $P_2O_5 \cdot 40\%\ Fe_2O_3$ containing UO_2, it was found [14] that only the FeO distances changed slightly, suggesting that U occupies voids in the FeOP network not altering the basic structure of the parent glass. It could be assumed that this is also valid for the present glass compositions. The property–composition fittings made above should be considered only as tentative ones owing to the very large variations in the chemical composition of the glasses and the complex expansion behavior for different T ranges. For $50 < T < 210/300\,°C$ [cycle T3], the negative contributions to the expansion produced by Na_2O, Fe_2O_3 and UO_2 would suggest that at least some proportions of each of those elements should occupy similar sites in the glass network. For instance, such proportions could bond strongly or more symmetrically the phosphate chains producing the compositional effects simulated by Eq. (1). In such T range, the lower expansion for CAB1 (compared to that for CAB2) could be attributed to the higher Fe content which would reduce α, according to Eq. (1), even if CAB1 does not contain Na_2O. For $400 < T < 470\,°C$ [cycle T4], this effect is apparently enlarged as CAB1 reduces further its α while for CAB2 (containing Na_2O) nearly no change in α, is detected. Now, for $T_g < T < T_{SOFT.}$, CAB1 expands much more than CAB2, and according to Eq. (4) such an effect can be explained by the higher Al_2O_3 content for CAB2 as compared to CAB1. The effect of Na_2O and Fe_2O_3 contents in Eq. (4) are considerably diminished relative to the case corresponding to Eq. (1). Obviously, the presence of Na_2O in CAB2 and its higher alumina content are responsible for the very different expansion behavior as compared to that for CAB1. It may be suggested that Na^+ goes into modifier positions but somehow remains chemically bonded to the phosphate chains and this situation applies up to $T_{SOFT.}$ Concerning the Fe ions and from the very high expansion for CAB1, for $T_g < T < T_{SOFT.}$, it could be suggested that either $Fe^{2+}OP$ or $Fe^{3+}OP$ bonds are lost when the glass approaches T_g causing the increase in expansion. For other glasses not containing Na_2O, as DR1 and DR2, the situation is close to that for CAB1 and $\alpha DR2 < \alpha DR1$, for $50 < T < (210-300)\,°C$, can be explained by Eq. (1) noting the much higher UO_2 level for DR2 as compared to that for DR1. Now,

for $T_g < T < T_{SOFT.}$, $\alpha DR1 \sim \alpha DR2$ which suggests similar liquids DR1 and DR2 with the U ions placed probably in voids of the liquid structure and being practically unbonded to the phosphate chains. For $T < T_g$ the U ions can be in interstitial sites strongly bonding the phosphate chains.

As a final comment, it should be noted that for PFeOx the short plateau at about 530 °C and the lower expansion for $530 \leqslant T \leqslant 548$ °C (Fig. 7; $h = 1$ °C min^{-1}) could be due to the oxidation of Fe^{2+} into Fe^{3+}, which would mean that the liquid-like iron–phosphate structure may also be strengthened when iron is present as Fe^{3+} ions.

Summarizing, the present glass compositions based on P-/Fe-oxides, having some of them important additions of Na_2O, Al_2O_3, and SiO_2, can dissolve significant quantities of UO_2 and still give quite stable glasses from the chemical durability and crystallization points of view. This suggests that these matrices are relevant for the immobilization of U radioactive wastes. From the basic science field, it is also made clear in this work that more systematic composition/property research is definitely needed to clearly sort out the final stability behavior of the present glasses containing UO_2. In that sense, measurements of glass viscosities, particularly at low temperatures with penetration and beam bending viscometers or through the fiber elongation method, should be performed on these types of glasses. Such characterization was found to be very useful to assess glass structural changes for T close to T_g for soda-lime–silica glasses around the $Na_2O \cdot 2CaO \cdot 3SiO_2$ composition [28].

5. Conclusions

The thermal expansion, T_g and $T_{SOFT.}$ of six glasses, having 56–66% P_2O_5, 14.8–34.2% Fe_2O_3 and 2–25 wt% additions of SiO_2, Al_2O_3, Na_2O and UO_2, were comparatively estimated from dilatometric measurements in similar conditions. The T_g reversibility was clearly verified by varying the heating rates between 1 and 5 °C min^{-1}. From linear fits of the various glass properties as functions of the six oxide components, it is suggested that the iron, sodium and uranium oxides decrease the thermal expansion (for $50 < T \leqslant 300$ °C), T_g and $T_{SOFT.}$. From fittings of the expansion data for $T > T_g$, it is obtained that the main controlling oxide additions are those of Al_2O_3 and Na_2O and the role of alumina content is reversed from the $T < T_g$ to the $T > T_g$ expansion ranges. It is suggested that Na^+, some of the Fe ions (probably Fe^{2+}) and U ions are placed in interstitial positions and are strongly bonding the phosphates chains for $T < 300$ °C. For $T > T_g$ it could be suggested that only Na^+ (and Al^{3+}) and perhaps Fe^{3+} remain well bonded to the phosphate structure.

From DTA/XRD analysis of the three glasses, it was confirmed that the crystallization tendency decreased with increasing the UO_2 level in the glasses. From DTA analysis of glasses CAB1 and DR1, it was obtained that the crystallization peaks shifted to higher temperatures, that is with increasing the UO_2 and Al_2O_3 contents.

Leaching test data for two compositions (PFeOx and PFeUOx) containing Na_2O suggests that the additions of UO_2 increase the chemical durability of such complex glasses.

Acknowledgments

This work is dedicated to the memory of Professor Peter Finlay James, who deceased on 2nd July, 2005.

References

1. F. Nicoletti and S. Hreglich, Inertisation of inorganic solid waste by vitrification; Proceedings of the 1st National Congress Valorisation and Recycling of Industrial Wastes; (Eds.), M. Pelino and G.C. Pellacani, E. Mucchi Editore, Italy (1998) 155–160.

2. M. Hidalgo, J. Ma. Rincón. Bol. Soc. Esp. Ceram. Vidr., 26 (1987), p. 227.

3. C.M. Jantzen. J. Non-Cryst. Solids, 84 (1986), p. 215.

4. J. Ma. Rincón, J. Cáceres, C. González Oliver, D.O. Russo, A. Petkova, H. Hristov. J. Therm. Anal. Calor., 56 (1999), p. 931.

5. M.G. Mesko, D.E. Day. J. Nucl. Mater., 273 (1999), p. 27.

6. D.E. Day, Z. Wu, C.S. Ray, P. Hrma. J. Non-Cryst. Solids, 241 (1998), p. 1.

7. T. Fukui, T. Ishinomori, Y. Endo, M. Sazarashi, S. Ono and K. Suzuki, Iron phosphate glass as potential waste matrix for high-level radioactive waste; WM 03 Conference, February 23–27, 2003, Tucson, AZ.

8. C-W Kim, D.E. Day. J. Non-Cryst. Solids, 331 (2003), p. 20.

9. M. Ijjaali, G. Venturini, R. Gerardin, B. Malaman, C. Gleitzer. Eur. J. Solid State Inorg. Chem., 28 (1991), p. 983.

10. ´Introduction to ceramics´; W.D. Kingery, H.K. Bowen, D.R. Uhlmann, John Wiley. 1976, p. 58.

11. N.C. Sturchio, M.R. Antonio, L. Soderholm, S.R. Sutton, J.C. Brannon. Science, 281 (1998), p. 971

12. G.K. Marasinghe, M. Karabulut, C.S. Ray, D.E. Day, M.G. Shumsky, W.B. Yelon, C.H. Booth, P.G. Allen, D.K. Shuh. J. Non-Cryst. Solids, 222 (1997), p. 144.

13. A. Moguš-Milanković, B. Pivac, K. Furić, D.E. Day. Phys. Chem. Glasses, 38 (2) (1997), p. 74.

14. M. Karabulut, G.K. Marasinghe, C.S. Ray, G.D. Waddill, D.E. Day. J. Appl. Phys., 87 (5) (2000), p. 2185.

15. S.T. Reis, M. Karabulut, D.E. Day. J. Nucl. Mater., 304 (2002), p. 87.

16. K.H. Chang, T.H. Lee, L.G. Hwa. Chin. J. Phys., 41 (4) (2003), p. 414.

17. A. Moguš-Milanković, M. Rajić, A. Drašner, R. Trojko, D.E. Day. Phys. Chem. Glasses, 39 (2) (1998), p. 70.

18. C.S. Ray, X. Fang, M. Karabulut, G.K. Marasinghe, D.E. Day. J. Non-Cryst. Solids, 249 (1999), p. 1.

19. I.W. Donald, B.L. Metcalfe and R.S. Greedharee, Crystallization kinetics of sodium iron aluminophosphate glasses studied by DSC and XRD; Proceedings of the XIX International Congress Glass, 2 Extended Abstracts Scotland (2001) 64–65.

20. D.O. Russo, D.S. Rodríguez, M. Sterba, J.Ma.L. Rincón, y C.J.R. González Oliver. Jornadas Sam/Conamet/AAS Argentina (2001), p. 835.

21. ASTM standard test method for determining chemical durability of nuclear waste glasses: the product consistency test (PCT). Designation C 1285 – 94.

22. D.O. Russo, D.S. Rodriguez, N. Grumbaum, y C.J.R. González Oliver. Jornadas Sam/Conamet/Simposio Materia Argentina (2003), p. 995.

23. C.J.R. González Oliver, D.O. Russo and A.F. Craievich, Iron phosphate glasses and gels; Activity Reports, LNLS Brasil 26th April 2005.

24. Ma.A. Villegas, J.Ma. Rincón L., D.O. Russo and C.J.R. González Oliver; Processing and characterization of vitreous matrices processed by melting and/or sol–gel for the immobilization of industrial and/or radioactive wastes; Varirei 2005 L´Aquila Italy 2005.

25. X. Yu, D.E. Day, G.J. Long, R.K. Brow. J. Non-Crystalline Solids, 215 (1997), p. 21.

26. A. Makishima, J.D. Mackenzie. J. Non-Crystalline Solids, 22 (1976), p. 305.

27. J.S. Jun, M.R. Cha, B.H. Jung, H.S. Kim. J. Kor. Ceram. Soc., 40 (11) (2003), p. 1127.

28. C.J.R. González Oliver, D.O. Russo, P.F. James. Phys. Chem. Glasses, 45 (2004), p. 100.